



## Cadaveric study of the ultrasound-guided erector spinae plane block over the transverse process of the twelfth thoracic vertebra in dogs: Transversal vs longitudinal approach

M.E. Herrera-Linares<sup>a,b,\*</sup>, B. Rico-Pérez<sup>b</sup>, D. Yaffy<sup>c</sup>, R. Fernández-Parra<sup>d</sup>, C. Llanos<sup>b</sup>, C. Parra-Martínez<sup>b</sup>, M.E. Herrera-Gutiérrez<sup>e</sup>, S. Sanchis-Mora<sup>d</sup>

<sup>a</sup> Doctoral School, Catholic University of Valencia San Vicente Mártir, San Agustín Square, 3, 46002, Spain

<sup>b</sup> Department of Clinical Science and Services. The Royal Veterinary College, Hawkshead Ln, Hatfield AL9 7TA, United Kingdom

<sup>c</sup> Department of Pathobiology and Population Sciences. The Royal Veterinary College, Hawkshead Ln, Hatfield AL9 7TA, United Kingdom

<sup>d</sup> Department of Small Animal Medicine and Surgery, Faculty of Veterinary Medicine and experimental Sciences, Catholic University of Valencia San Vicente Mártir, Valencia, C/ de Quevedo, 2, 46001, Spain

<sup>e</sup> Department of Intensive Care Medicine. Regional University Hospital of Málaga, Av., 84, Málaga 29010, Spain

### ARTICLE INFO

#### Keywords:

Analgesia  
Anatomy  
Dog  
Regional anesthesia  
Ultrasound

### ABSTRACT

This study describes a transversal (TV) ultrasound-guided erector spinae plane (ESP) block technique over the transverse process of T12. And evaluates the distribution of the dye and affected nerves branches compared to a longitudinal (LNG) approach over the transverse process of T12 in canine cadavers. Secondly, it also compares de anatomy and dimensions of the transverse processes of T12 with T9 and T5. For this double-masked, cadaveric experimental study, 12 adult Beagle cadavers were injected with 0.6 mL/kg of dye/contrast. Spread was evaluated by computed tomography (CT) and dissection.

Mean bodyweight was 9.76 ( $\pm 0.59$ ) kg. The TV and LNG approaches stained a median (range) of four (2–6) and three (1–6) medial branches of the dorsal rami of the spinal nerves, three (2–6) and three (2–5) lateral branches, and one (0–3) and one (0–4) ventral branches, respectively. Dye was detected in the epidural space in 55.6% and 66.7% of cases for the TV and LNG approaches, respectively ( $P=0.63$ ). And in the ventral paravertebral compartment in 22.2% and lymphatics in 88.8% in both approaches. There were no statistical differences for the spread. The dorsolateral edge of the transverse process (TP) was not visible with CT at T12. The mean ( $\pm$ SD) length of the TP was significantly shorter at T12 [3.34 ( $\pm 0.22$ )] mm, compared to T9 [6.08 ( $\pm 0.47$ )] mm and T5 [5.93 ( $\pm 0.62$ )] mm ( $P < 0.001$ ). This study showed similar distribution whether using a TV or LNG approach and differences in the anatomy and length of the T12 TP.

### Introduction

The erector spinae plane (ESP) block is an interfascial plane block first reported in humans by Forero et al. (2016). In canine cadavers, this block consistently stains the dorsal rami of the thoracic spinal nerves and their lateral (LBDR) and medial branches (MBDR), providing innervation to the dorsolateral aspect of the spine (Ferreira et al., 2019; Portela et al., 2020; Medina-Serra et al., 2021; Cavalcanti et al., 2022). While various theories suggest additional sites of action in humans (Chin et al., 2019; Chin and El-Boghdady, 2021), none have been confirmed in dogs. Furthermore, the clinical application of ESP for managing perioperative pain in dogs is supported by several studies (Zannin et al.,

2020; Bartholomew and Ferreira, 2021; Gómez Fernández et al., 2021; Portela et al., 2021)."

The erector spinae muscles are part of the epaxial musculature. They include the iliocostalis, spinalis and the longissimus muscles situated on the dorsolateral aspect of the vertebrae and ribs (Portela et al., 2020). The thoracic ultrasound (US)-guided ESP block in dogs and humans has been originally performed with a longitudinal (LNG) parasagittal approach (Forero et al., 2016; Ferreira et al., 2019; Portela et al., 2020). In human medicine, benefits of the transversal (TV) approach has been described including improved detection of inadvertent intramuscular injections, and better localization of the area, plus an additional approach if the LNG ESP was previously performed intramuscularly

\* Corresponding author at: Doctoral School, Catholic University of Valencia San Vicente Mártir, San Agustín Square, 3, 46002, Spain.

E-mail address: [manuelherreralinares@gmail.com](mailto:manuelherreralinares@gmail.com) (M.E. Herrera-Linares).

<https://doi.org/10.1016/j.tvjl.2024.106094>

Received 28 August 2023; Received in revised form 4 March 2024; Accepted 4 March 2024

Available online 5 March 2024

1090-0233/© 2024 The Authors. Published by Elsevier Ltd. This is an open access article under the CC BY license (<http://creativecommons.org/licenses/by/4.0/>).

(Hruschka and Arndt, 2018; Narayanan and Venkataraju, 2019; Sharma et al., 2020). A canine study compared a TV approach perpendicular to the mamillary process with the LNG parasagittal approach over the transverse process at the thoracic vertebra T12. The TV approach provided a more reliable coverage of the MBDR compared to LBDR in dogs with a mean weight of 24.4 ( $\pm 11.5$ ) kg (Cavalcanti et al., 2022).

In veterinary medicine, the ESP block is predominantly used to provide perioperative analgesia in patients undergoing spinal surgery (Portela et al., 2021). Intervertebral disk disease (IVDD) most commonly affects the T12-T13 and T13-L1 disks in dogs weighing between 5.6 and 12.3 kg, with an 80% incidence in dogs under 15 kg (Aikawa et al., 2012; Klesty et al., 2019). These thoracic vertebrae have marked anatomical differences, including a reduced transverse process size (Evans and de Lahunta, 2013a), which may affect the difficulty of this block.

The aim of this study was to describe and assess the nerve staining and distribution of a novel US-guided ESP block technique using a TV approach on the dorsal surface of the transverse process of T12, and to compare it to a LNG approach on the same area in cadavers with a similar weight to dogs susceptible to IVDD at this level. The second objective was to measure and compare the lengths and anatomy of the transverse processes of T5, T9, and T12 using CT image analysis. We hypothesized that both the TV and LNG approaches would result in similar nerve staining and distribution.

## Materials and methods

The study was conducted under the ethical approval of the Royal Veterinary College (Approval number, URN 2018 1771-3; Approval date, 25 January 2018).

### Animals

Twelve adult Beagle cadavers without a history of thoracolumbar injury were thawed for 48 hours at room temperature before the commencement of this study. Three were used for a preliminary anatomical study, while nine were used to compare the traditional LNG approach with our TV approach.

### Preliminary anatomical study

Three cadavers were examined using CT, US, and dissection to investigate anatomical landmarks and differences in the thoracolumbar epaxial muscular region, and to identify the medial and lateral branches of the dorsal rami and ventral branches of the spinal nerves.

Thoracic and abdominal CT scans were conducted and evaluated by a diagnostic imaging resident. CT studies were acquired using a 320-slice multidetector CT scanner (Canon Aquilion ONE/GENESIS; Toshiba Medical Systems). The images were obtained in a 512 $\times$ 512 matrix with a medium frequency reconstruction algorithm (120 kVp, 90 mAs, 1 mm slice thickness). The studies were retrospectively reviewed on a digital workstation using an online DICOM viewer (eUnity, Mach7 Technologies).

The ultrasound was performed by an anesthesia resident. A 15–6 MHz linear transducer connected to an SII Sonosite ultrasound machine (SonoSite Inc.) was used to study the landmarks of interest for the TV approach in the previously clipped T12 area.

A pathology resident performed the anatomical dissections. Following a longitudinal dorsal midline incision, the thoracolumbar superficial muscles and fascia from T1 to L4 were dissected. The exposed erector spinae muscles and intermuscular fascia were dissected to expose the LBDR and MBDR. The external and internal intercostal muscles were dissected to expose the ventral branches of the spinal nerves (VBSN). The sympathetic trunk and paravertebral space were exposed following removal of the thoracic and abdominal viscera through a ventral midline incision.

### Ultrasound-guided LNG and TV ESP injection

Nine dogs were randomly assigned (<https://www.randomizer.org>) the approach (LNG or TV) and injection sites (left or right of the midline). All the injections were performed by a first (TV) and second year anesthesia resident (LNG).

The linear transducer was used to inject a 1:1 solution of methylene blue dye (methylthioninium chloride Injection 1% w/v; Martindale Pharmaceuticals Ltd.) and iohexol (Omnipaque 300; GE Healthcare) radiographic contrast, totaling 0.6 mL/kg, bilaterally into each cadaver.

Each cadaver was placed in sternal recumbency, and the dorsum was clipped. In the LNG group, ultrasound identified the 12th rib by counting from the last rib. The transducer was then moved medially to identify the irregular hyperechoic shape of the transverse process of T12. Using an in-plane technique, a 22-gauge, 80 mm echogenic insulated needle (Ultrplex 360 needle, BBraun Medical Ltd.) was advanced through the erector spinae musculature in a craniodorsal-to-caudoventral direction until the tip was in contact with the dorsal aspect of the transverse process (Fig. 1a, b and c). The tip of the needle was slightly forced against the bone to ensure it passed through the last layer of the muscle, and the solution was injected as rapidly as possible.

For the TV approach, the transducer was positioned caudal to the last rib in the midline, perpendicular to the spine, and slightly tilted laterally. The probe was then moved cranially until the rounded bony shadow of the 12th rib appeared on the lateral aspect of the image. It was followed latero-medially until it contacted the hyperechoic surface of the T12 transverse process. This positioning clearly visualized the lamina and transverse process of the vertebrae, the costotransverse joint, and the tubercle of the rib in the ultrasound image, thus facilitating precise identification of the injection site. Using an in-plane technique, the needle was advanced in a dorsolateral-to-ventromedial direction until the tip reached the dorsal aspect of the transverse process just beyond the costotransverse joint (Fig. 1d, e, and f). To ensure penetration through the last layer of muscle, the needle tip was pressed against the bone. The same volume of dye/contrast solution was then injected, at the same speed, at this precise point.

### CT study and anatomical dissection

Immediately after injections, cadavers were positioned in sternal recumbency, and a thoracolumbar CT was performed by the diagnostic imaging resident, who was blinded to the treatment. The length of the transverse process and the presence of the dorsolateral edge of the transverse process at T12, T9, and T5 were recorded. The length of the spread in the ESP, epidural, paravertebral, and lymphatic spaces, were recorded and compared between both approaches.

Immediately after the CT scans, the cadavers were moved to the postmortem room. The dogs were dissected sequentially, as described above, by the same pathologist who was blinded to the treatment. The distribution of the dye solution with respect to the MBDR, LBDR, VBSN, and paravertebral structures was compared between the two approaches. Successful staining of the MBDR, LBDR, and VBSN was defined when the dye solution was circumferentially distributed by more than 1 cm (Portela et al., 2017). The craniocaudal length of the spread was measured, with each vertebra treated as a unit. Successful staining of a vertebra was confirmed when the solution effectively covered more than 50% of the entire length of the vertebral body (Son et al., 2011).

### Statistical analysis

Data were analyzed masked to group allocation using IBM SPSS Statistic for macOS v. 28.0 (IBM Corp.). The results are shown as *n* (%) or median (range) for non-parametric data and mean ( $\pm$ SD) for parametric data. For comparison, we performed a univariate analysis with the Fisher exact test for categorical variables and non-parametric tests for

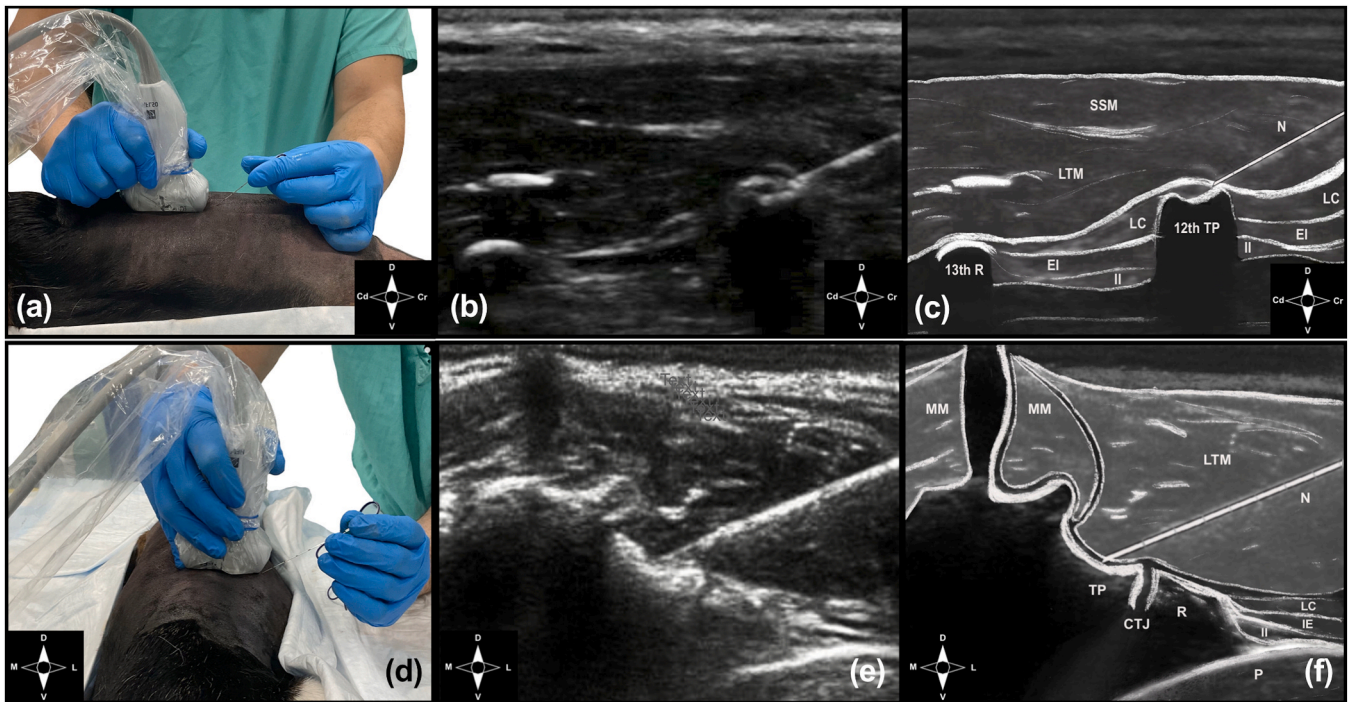


**Fig. 1.** Ultrasound-guided erector spinae plane (ESP) block at T12. Technique, images, and landmarks of the longitudinal (LNG) and transversal (TV) approaches. (a) External view of the LNG approach for the ESP with the orientation of the US transducer and the needle direction. (b) Ultrasound image of the LNG approach of the ESP with the needle in position on the injection area. (c) Schematic representation of (b). (d) External view of the TV approach for the ESP with the orientation of the US transducer and the needle direction in position on the injection area. (e) Ultrasound image of the TV approach of the ESP. (f) Schematic representation of (e). Cd, caudal; Cr, cranial; CTJ, costotransverse joint; D, dorsal; IE, external intercostal muscle; II, internal intercostal muscle; L, lateral; LC levatores costarum muscle; LTM longissimus thoracis muscle; M, medial; MM, multifidus muscle; N, needle; P, pleura; TP, transverse process of the twelfth thoracic vertebrae; R, tubercle of the rib; V, ventral.

continuous variables (u-Mann Whitney comparing two groups and Kruskal-Wallis test comparing more than two groups). Differences were considered significant when the *P*-value was <0.05. The sample size was based on similar studies (Portela et al., 2020; Cavalcanti et al., 2022).

## Results

### Ultrasound-guided LNG and TV ESP injection

The mean bodyweight of the nine cadavers was 9.76 ( $\pm 0.59$ ) kg with a body condition score of 6/9. Each group (TV and LNG) received a total of nine injections. Anatomical landmarks were identified in all cases, and the needle was visualized at the T12 level before injections.

### Spread of the injectate

A cranio-caudal distribution of the injected solution was observed through the interfascial ESP in both CT and dissection. The spread was predominantly ventromedial to the longissimus and semispinalis muscles cranial to the injection and laterodorsal caudally. There were no statistically significant differences between the TV and LNG groups.

The length of the spread recorded during the dissection was four (3–6) and four (4–7) vertebrae for the TV and LNG approaches. Across all cadavers, the most cranial and caudal stained vertebrae were T9 and L1, and T8 and L3, in the TV and LNG groups, respectively. Based on the CT images, the length of the spread was eight (5–9) and seven (5–8) vertebrae in the TV and LNG groups, respectively. The most cranial and caudal vertebrae reached were T8 and L2, and T7 and L3, in the TV and LNG groups, respectively (Fig. 2). Differences in CT and dissection spread were statistically significant for TV (*P* = 0.003) and LNG (*P* = 0.004).

Dissections revealed multisegmental spread along the ESP in all the

injections. The TV and LNG groups stained a median of four (2–6) and three (1–6) MBDR, respectively, and three (2–5) and three (2–6) LBDR, respectively. Across all cadavers, the most cranial and caudal MBDR and LBDR stained were T9 and L1, and T8 and L3, in the TV and LNG groups, respectively (Fig. 2). Complete staining of the VBSN within the dorsal paravertebral compartment was recorded in all treatments, except for one per group (88.9%) (Fig. 2). The TV and LNG approaches stained one (0–3) and one (0–4) VBSN, respectively. Ventral paravertebral compartment distribution was recorded in two cadavers (22.2%) per group (Figs. 2 and 3b and d). The distribution and staining of the dorsal rami of the spinal nerves were not assessed due to difficulties in identification.

CT analysis showed lymphatic spread through the thoracic duct in eight (88.8%) cadavers, with a median spread of six (0–11) vertebrae (Figs. 2 and 5a and c) with spread from both approaches. Epidural distribution occurred in five (55.6%) and six (66.7%) cadavers in the TV and LNG approach, respectively (Figs. 2 and 3b). The median of the epidural spread was one (0–12) vertebrae for both groups. The thoracic sympathetic ganglion at the T12 level was fully stained in one (11.1%) injection in the LNG group and partially stained in one (11.1%) in the TV group. Paravertebral distribution of contrast was identical to the dissection dye distribution.

### Anatomical study

The anatomical study, CT and US scan showed anatomical differences between T12 and T9/T5. The dorsolateral edge of the transverse process was not visible at T12 (Fig. 4). The mean length of the transverse process was 3.34 ( $\pm 0.22$ ) mm at T12, 6.08 ( $\pm 0.47$ ) mm in T9, and 5.93 ( $\pm 0.62$ ) mm in T5. There was a statistical difference between T12 with T9 and T5 (*P* < 0.001). There were no statistically significant differences between T9 and T5 (*P* = 0.33).

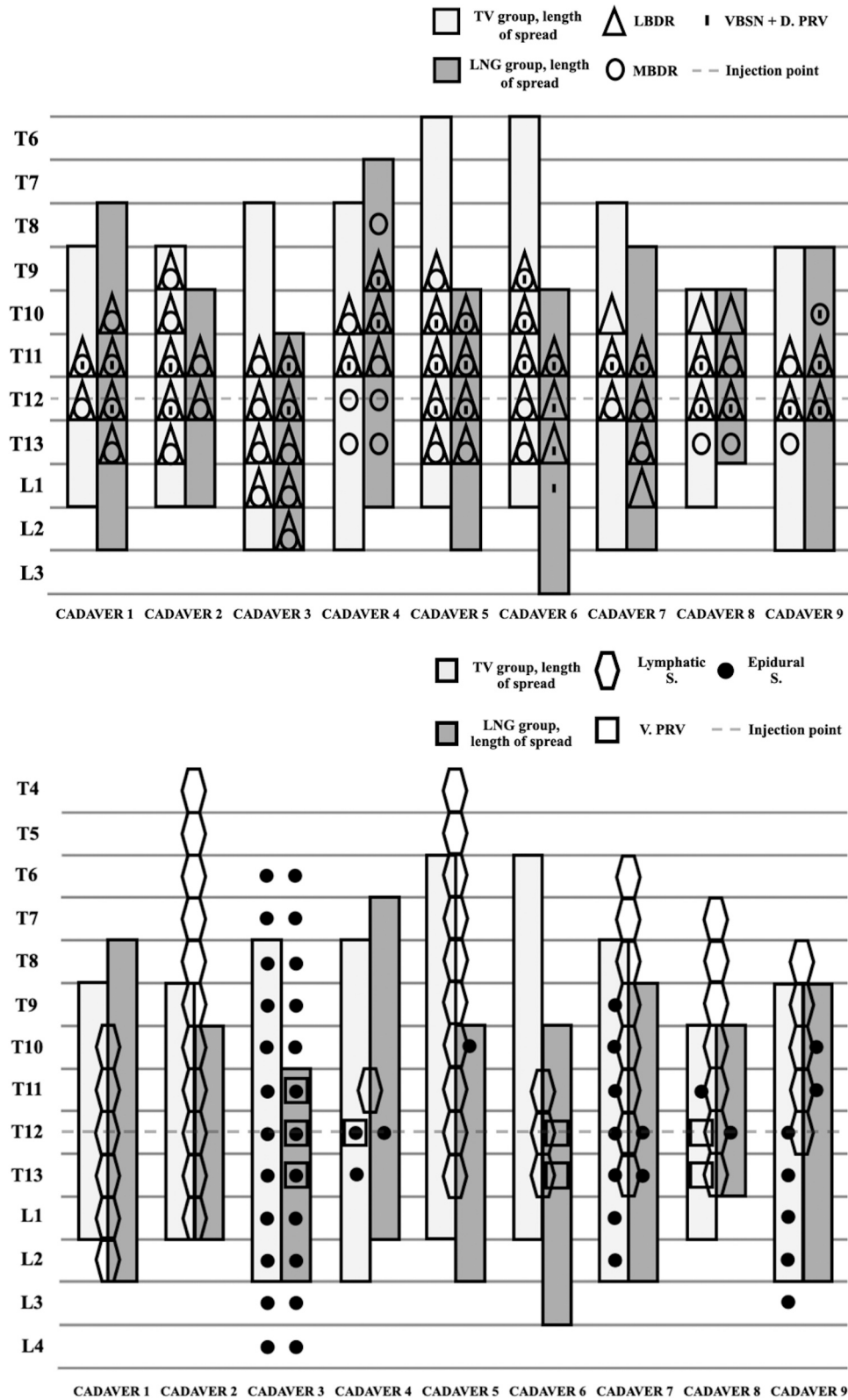


**Fig. 2.** Length of the spread using a transversal (TV) and a longitudinal (LNG) approach of the erector spinae block at T12 level in each cadaver. Dye of the lateral branches of the dorsal rami of the spinal nerves (LBDR), medial branches of the dorsal rami of the spinal nerves (MBDR) and ventral branches of the spinal nerves (VBSN) and spread of the dye in the lymphatic system (Lymphatic s.), epidural space (Epidural s.), dorsal and ventral paravertebral spaces (D. PRV; V. PRV). L, lumbar vertebra T, thoracic vertebra.

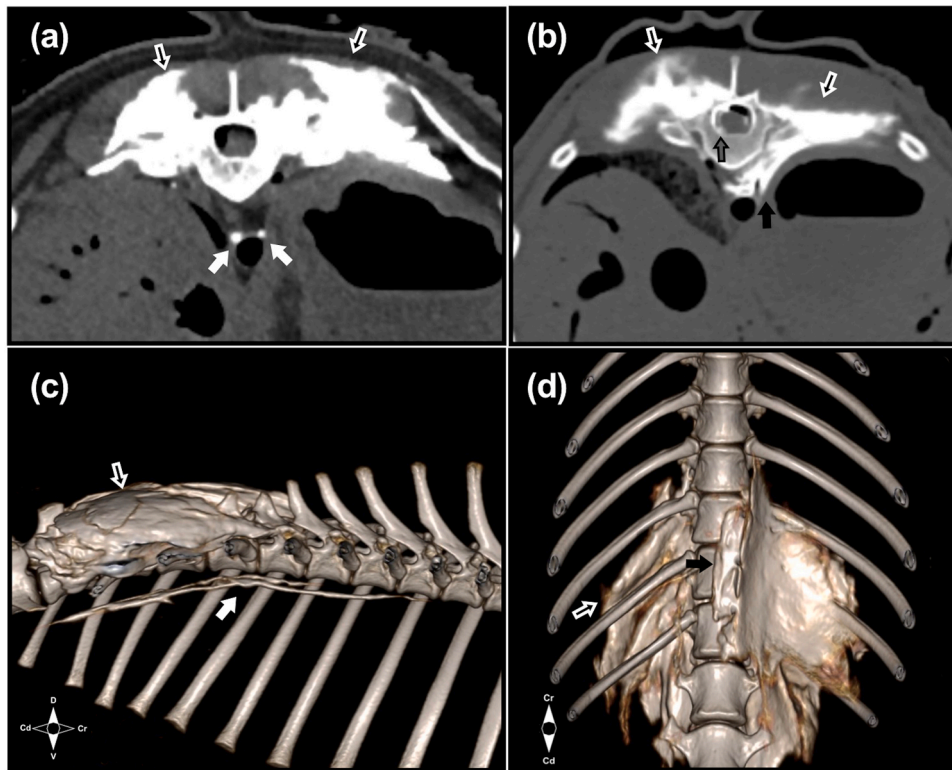


**Fig. 3.** Computed tomography (CT) imaging study showing the spread of the contrast/dye solution after the erector spinae plane (ESP) block. (a,b) Transverse CT images showing spread in the ESP (white and black arrow), lymphatic thoracic duct (a, white arrow), paravertebral space (b, black arrow) and inside the epidural space (b, black and grey arrow). (c,d) Representative 3D rendering of the CT imaging study showing spread in the ESP (white and black arrow), lymphatic thoracic duct (c, white arrow) and paravertebral space (d, black arrow). Cd, caudal; Cr, cranial; D, dorsal; V, ventral.

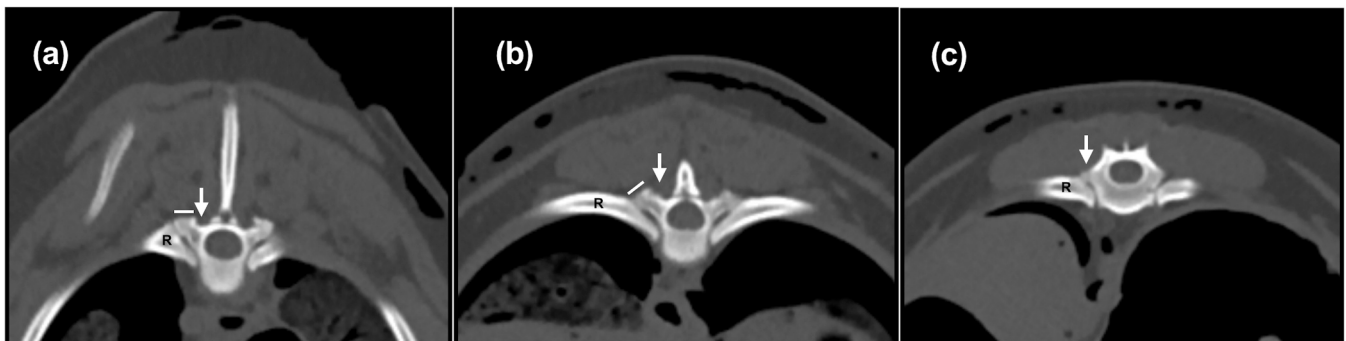


**Fig. 4.** Transverse CT scan at (a) T5, (b) T9 and (c) T12 level showing the costotransverse joint and the transverse process. Length of the dorsolateral edge of the transverse process (white line). Dorsal aspect of the transverse process (white arrow). R, rib.

Dissection of the erector spinae muscles revealed fusion of the two layers of the thoracolumbar fascia, which anchored and passed between the longissimus thoracis and iliocostalis thoracis muscles and attached laterally and dorsally to the vertebral transverse and spinous processes, respectively. The longissimus thoracis muscle formed the bulk of the erector spinae muscles dorsal to the deep thoracolumbar fascia. The longissimus muscles were over the proximal aspect of the ribs and the levatores costarum muscles where they inserted on the accessory, vertebral processes. The rotatores and multifidus muscles covered the vertebral groove, with the multifidus muscles continued medially and inserted on the transverse process of T12 before progressing caudodorsally.

In the examined cadavers, the dorsal rami were divided into MBDR and LBDR between the multifidus and levatores costarum muscles (Fig. 5a). The MBDR followed a caudodorsal trajectory between the

longissimus thoracis muscle and the vertebra lamina or multifidus muscles. The LBDR passed between the longissimus thoracis and the dorsal surface of the iliocostalis thoracis and the levatores costarum, and exited the ESP as cutaneous nerves through the thoracolumbar fascia laterally. The VBSN traversed laterally and ventrally within intercostal spaces and muscles.

#### Discussion

The injection of 0.6 mL/kg of dye solution using either TV or LNG approaches at the T12 level showed a similar degree of nerve staining, longitudinal spread through the ESP and epidural, lymphatic, and paravertebral distribution.

The dorsolateral edge of the transverse process is a crucial landmark for the LNG ESP injection, preventing inadvertent injection under the

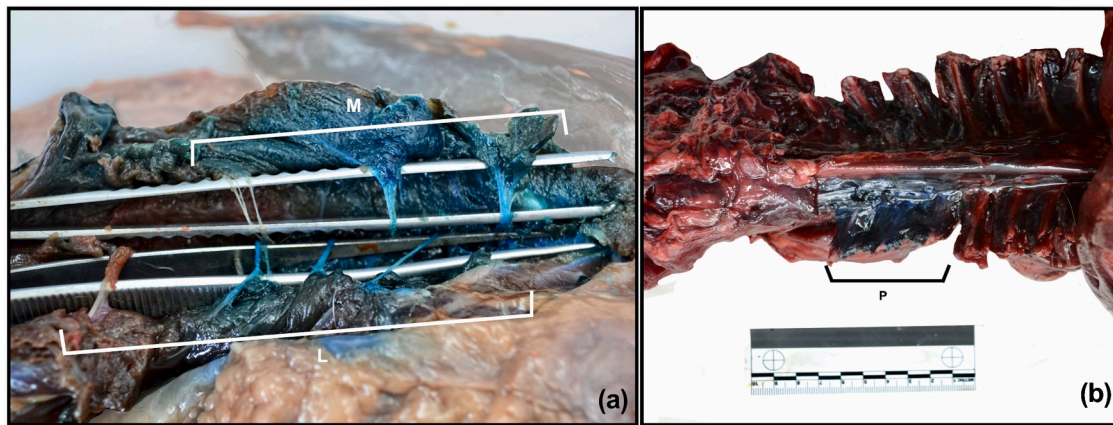


**Fig. 5.** Images of the anatomical dissection after erector spinae plane (ESP) block with methylene blue (Methylthioninium Chloride Injection 1% w/v; Martindale Pharmaceuticals Ltd, UK) dye solution and iohexol (Omnipaque 300; GE Healthcare, UK). (a) Medial (isolated dorsally in the image) and lateral (isolated ventrally in the image) branches of the dorsal rami of the spinal nerves. (b) Ventral view of the thorax showing paravertebral spread of the dye solution after removing the ventral and lateral attachments of the diaphragm, sternum, and thoracic and abdominal viscera. M, medial branches of the dorsal rami of the spinal nerves; L, lateral branches of the dorsal rami of the spinal nerves; P, paravertebral spread.

multifidus muscles and averting abnormal spread (Portela et al., 2020; Cavalcanti et al., 2023). Our study revealed a significant decrease in the size of the transverse process at the caudal thoracic vertebrae, with the dorsolateral edge notably absent at T12 (see Fig. 2). However, compared to the cranial thoracic region, the caudal thoracic region exhibited dorsomedial positioning of the multifidus muscles. This study's findings, similar to those of other studies in the cranial thoracic region (Portela et al., 2020), alongside the absence of multifidus muscles near the injection site, suggest that the lack of a dorsolateral edge on the T12 transverse process did not affect the injectate spread.

The TV approach in humans may improve detection of an inadvertent injection into erector spinae muscle compared to the LNG approach (Hruschka and Arndt, 2018; Narayanan and Venkataraju, 2019; Sharma et al., 2020). At T12 in dogs, the decreased length of the transverse process may hinder the LNG approach. Moreover, small lateral or medial movement of the probe could display the rib or lamina surface instead. If these structures are mistaken as the surface of the transverse process, the solution might be misplaced and the spread altered. A transversal approach obtains a cross-sectional view of the area. Therefore, the lamina and transverse process of the vertebrae, the costotransverse joint, and the tubercle of the rib are present in the ultrasound image, facilitating the recognition of the area of injection. In this case, small lateral or medial movements of the probe would displace these structures out of the image, reducing the risk of misplacement. In this study, the results were similar between approaches. However, this study did not aim to compare the quality of landmark visibility or the benefits of performing a TV or LNG approach. Therefore, the benefits of each technique cannot be ascertained, and further studies are needed to evaluate it.

The CT exhibited significantly greater longitudinal spread into the ESP than the dissection [TV ( $P = 0.003$ ); LNG ( $P = 0.004$ )]. The spread towards the ESP changed from medioventral to laterodorsal caudally, surrounding the longissimus thoracis and semispinalis muscles. The LBDR and MBDR are ventromedially to the longissimus thoracis muscle within the ESP. Consequently, to evaluate the nerve dye, the dissection focused on this region, thus explaining the different results of the length of the spread. Additionally, a CT assessment was included due to the potential local effect if an anesthetic drug was used, which could enhance analgesia even when there is no direct involvement of spinal nerves (Grubb & Lobprise, 2020).

Following anatomical dissection, we found that both MBDR and LBDR dyes exhibited no differences irrespective of the approach, yielding similar results to those reported by Portela et al. (2020) at the T9 level with an LNG approach. However, the number of dyed branches was slightly higher than Cavalcanti et al. (2021) at T12 in the transverse

or the mammillary processes. These differences in outcomes compared to Cavalcanti et al. (2021) could be attributed to the larger volume employed in our study.

In contrast to similar studies in dogs, we observed the dye of the VBSN and epidural, paravertebral, and lymphatic spread, together with the LBDR and MBDR (Ferreira et al., 2019; Portela et al., 2020; Cavalcanti et al., 2022). There are a few theories in human medicine regarding this spread towards other compartments (Chin et al., 2019). The thoracolumbar fascia and the intertransverse connective tissue are perforated by the dorsal rami of the spinal nerves and the vessels that join these nerves (Evans and de Lahunta, 2013b; Portela et al., 2020). These perforations and the costotransverse foramen, joint and ligaments may create areas of low resistance that are permeable to liquids (Chin et al., 2019). In horses, paravertebral and epidural spread have been reported when the ESP was performed at T16 (Delgado et al., 2021). Similarly to Delgado et al. (2021), the injection site in our study was at the thoracolumbar region, spanning the transitional area between the thoracic and lumbar spine from T11 to L2 in dogs. The anatomical changes in the thoracolumbar area, such as the reduced length of the transverse process, absence of the intercapital ligament, and transition between the thoracic and lumbar epaxial musculature, could potentially enhance the permeability of these areas of low resistance to fluids (Haussler, 1999; Coates, 2000; Evans and de Lahunta 2013b). However, Cavalcanti et al. (2021) only reported LBSN and MBSN dye using the LNG approach at T12 with the same area of injection. The average weight of the cadavers in Cavalcanti's study was 24.4 ( $\pm 11.5$ ) kg, while the mean weight in our study was smaller. In humans, pediatrics cadaveric studies have shown that the smaller area of the patient and the differences in paravertebral and intertransverse connective tissue and muscle thickness may improve the spread of this block (Govender et al., 2020). Moreover, Cavalcanti et al. (2021) investigated the spread with a cadaveric dissection alone while in our study a CT evaluation was added to the cadaveric dissection to improve the assessment of the spread (Medina-Serra et al., 2021). Differences in these results could thus be due to differences in body weight, volume, and CT evaluation.

Unexpectedly, an epidural spread of 12 vertebrae was found in one cadaver. The cause of this spread remains unclear to the authors. Potential factors, such as individual undiagnosed anatomical or post-mortem variations, or dispersion into the epidural canal following a bilateral accidental paravertebral injection, though improbable, cannot be ruled out. These outcomes might contribute to complications in a clinical setting, resulting in partial femoral motor block or cardiovascular depression (Steagall et al., 2017). A comparable extended epidural spread has also been found in humans (De Cassai et al., 2020).

Lymphatic spread has not been reported in humans or canines. A study on live pigs revealed lymphatic distribution of the dye solution during post-mortem (Otero et al., 2020). Reports in humans and rabbits also indicate post-mortem lymphatic drainage (Suami et al., 2005; Shinaoka et al., 2020). This could explain the observed lymphatic spread in our study, even when using cadavers. Considering the multidimensional role of the immune system in pain and inflammation (Verma et al., 2015), this spread could contribute to enhance the analgesic effect of this block.

This study has several limitations. Each technique was executed by a different operator, potentially introducing operator bias. Although both operators underwent similar training for the LNG approach, only one had prior knowledge of the landmarks of the TV technique. Consequently, to optimize results within the limited sample size, each operator followed a different approach. Additionally, post-mortem changes may have affected the distribution of dye compared to the spread of local anesthetics in living patients. Finally, the CT scan was conducted after both techniques had been completed on the same cadaver. As a result, evaluation of the spread into the epidural and lymphatic canal for each approach was limited.

## Conclusions

This study highlights the potential of the TV approach as an alternative to the LNG, achieving comparable multisegmental dye distribution through the erector spinae interfascial plane. Spread of the VBSN, epidural and paravertebral spaces, lymphatic system, and sympathetic chain was observed. The findings revealed a smaller size of the transverse process and the absence of its dorsolateral edge at the T12 level in Beagles compared to cranial thoracic vertebrae, which did not affect the injectate spread. Further research is however essential to fully evaluate the effectiveness of this approach and to understand the potential impact of weight and anatomical differences on US-guided ESP blocks.

## Conflict of interest statement

None of the authors has any financial or personal relationships that could inappropriately influence or bias the content of the paper.

## Acknowledgements

Preliminary results were presented as an Abstract at the XVII Congress of the Spanish Anesthesia and Analgesia Veterinary Society (SEAAV), Granada, 1–3 June 2023.

## References

- Aikawa, T., Fujita, H., Kanazono, S., et al., 2012. Long-term neurologic outcome of hemilaminectomy and disk fenestration for treatment of dogs with thoracolumbar intervertebral disk herniation: 831 cases (2000-2007). *J. Am. Vet. Med. Association* 241, 1617–1626.
- Bartholomew, K.J., Ferreira, T.H., 2021. Ultrasound-guided erector spinae plane block as part of a multimodal analgesic approach in a dog with acute pancreatitis. *Vet. Anaesth. Analgesia* 48, 629–632.
- Cavalcanti, M., Teixeira, J.G., Medina-Serra, R., et al., 2022. Erector spinae plane block at the thoracolumbar spine: a canine cadaveric study. *Vet. Anaesth. Analgesia*.
- Chin, K.J., Adhikary, S.D., Forero, M., 2019. Erector Spinae Plane (ESP) Block: a new paradigm in regional anesthesia and analgesia. *Current Anesthesiol. Rep.* 9, 271–280.
- Chin, K.J., El-Boghdady, K., 2021. Mechanisms of action of the erector spinae plane (ESP) block: a narrative review. *Can. J. Anaesthesia* 68, 387–408.
- Coates, J.R., 2000. Intervertebral disk disease. *Vet. Clin. North America: Small Animal Pract.* 30, 77–110.
- De Cassai, A., Fasolo, A., Geraldini, F., et al., 2020. Motor block following bilateral ESP block. *J. Clin. Anesth.* 60, 23.
- Delgado, O.B.D., Louro, L.F., Rocchigiani, G., et al., 2021. Ultrasound-guided erector spinae plane block in horses: a cadaver study. *Vet. Anaesth. Analgesia* 48, 577–584.
- Evans, H.E., de Lahunta, A., 2013a. Chapter 4: The Skeleton. In: Evans, H., de Lahunta, A. (Eds.), *Miller's Anatomy of the Dog*, Fourth edn. Elsevier Saunders, St. Louis, MO, USA, pp. 80–157.
- Evans, H.E., de Lahunta, A., 2013b. Chapter 6: The Muscular System. In: Evans, H., de Lahunta, A. (Eds.), *Miller's Anatomy of the Dog*, Fourth edn. Elsevier Saunders, St. Louis, MO, USA, pp. 185–208.
- Ferreira, T.H., St James, M., Schroeder, C.A., et al., 2019. Description of an ultrasound-guided erector spinae plane block and the spread of dye in dog cadavers. *Vet. Anaesth. Analgesia* 46, 516–522.
- Forero, M., Adhikary, S.D., Lopez, H., et al., 2016. The Erector Spinae Plane Block: A Novel Analgesic Technique in Thoracic Neuropathic Pain. *Reg. Anesth. Pain Med.* 41, 621–627.
- Gómez Fernández, L., Huuskonen, V., Potter, J., 2021. The combination of an ultrasound-guided erector spinae plane (ESP) block and epidural morphine as effective intra-operative adjuncts to opioid premedication in six dogs undergoing lateral thoracotomy. *Vet. Record Case Rep.* 9.
- Govender, S., Mohr, D., Bosenberg, A., et al., 2020. The anatomical features of an ultrasound-guided erector spinae fascial plane block in a cadaveric neonatal sample. *Paediatric Anaesth.* 30, 1216–1223.
- Grubb, T., Lobprise, H., 2020. Local and regional anaesthesia in dogs and cats: Descriptions of specific local and regional techniques (Part 2). *Vet. Med. Sci.* 6, 218–234.
- Haussler, K.K., 1999. Anatomy of the thoracolumbar vertebral region. *Vet. Clin. North America: Equine Pract.* 15, 13–26.
- Hruschka, J.A., Arndt, C.D., 2018. Transverse Approach to the Erector Spinae Block. *Reg. Anesth. Pain Med.* 43, 805.
- Klesty, A., Forterre, F., Bolln, G., 2019. Outcome of intervertebral disk disease surgery depending on dog breed, location and experience of the surgeon: 1113 cases]. *Tierärztlich-Praxis Ausgabe K Kleintiere Heimtiere* 47, 233–241.
- Medina-Serra, R., Foster, A., Plested, M., et al., 2021. Lumbar erector spinae plane block: an anatomical and dye distribution evaluation of two ultrasound-guided approaches in canine cadavers. *Vet. Anaesth. Analgesia* 48, 125–133.
- Narayanan, M., Venkataraju, A., 2019. Transverse approach to the erector spinae block: is there more? *Reg. Anesth. Pain Med.* 44, 529.
- Otero, P.E., Fuensalida, S.E., Russo, P.C., et al., 2020. Mechanism of action of the erector spinae plane block: distribution of dye in a porcine model. *Reg. Anesth. Pain Med.* 45, 198–203.
- Portela, D.A., Campoy, L., Otero, P.E., et al., 2017. Ultrasound-guided thoracic paravertebral injection in dogs: a cadaveric study. *Vet. Anaesth. Analgesia* 44, 636–645.
- Portela, D.A., Castro, D., Romano, M., et al., 2020. Ultrasound-guided erector spinae plane block in canine cadavers: relevant anatomy and injectate distribution. *Vet. Anaesth. Analgesia* 47, 229–237.
- Portela, D.A., Romano, M., Zamora, G.A., et al., 2021. The effect of erector spinae plane block on perioperative analgesic consumption and complications in dogs undergoing hemilaminectomy surgery: a retrospective cohort study. *Vet. Anaesth. Analgesia* 48, 116–124.
- Sharma, S.K., Mistry, T., Ahmed, S., 2020. Ultrasound-guided thoracic erector spinae plane block: A modified transverse approach. *Saudi J. Anaesth.* 14, 142–143.
- Shinaoka, A., Koshimune, S., Suami, H., et al., 2020. Lower-Limb Lymphatic Drainage Pathways and Lymph Nodes: A CT Lymphangiography Cadaver Study. *Radiology* 294, 223–229.
- Son, W.G., Kim, J., Seo, J.P., et al., 2011. Cranial epidural spread of contrast medium and new methylene blue dye in sternally recumbent anaesthetized dogs. *Vet. Anaesth. Analgesia* 38, 510–515.
- Suami, H., Taylor, G.I., Pan, W.R., 2005. A new radiographic cadaver injection technique for investigating the lymphatic system. *Plastic Reconstruct. Surg.* 115, 2007–2013.
- Steagall, P.V.M., Simon, B.T., Teixeira Neto, F.J., et al., 2017. An Update on Drugs Used for Lumbosacral Epidural Anesthesia and Analgesia in Dogs. *Front. Vet. Sci.* 4, 68.
- Verma, V., Sheikh, Z., Ahmed, A.S., 2015. Nociception and role of immune system in pain. *Acta Neurol. Belgica* 115, 213–220.
- Zannin, D., Isaka, L.J., Pereira, R.H., et al., 2020. Opioid-free total intravenous anesthesia with bilateral ultrasound-guided erector spinae plane block for perioperative pain control in a dog undergoing dorsal hemilaminectomy. *Vet. Anaesth. Analgesia* 47, 728–731.